[Contribution from the Gates and Crellin Laboratories of Chemistry,[5] California Institute of Technology

Radiation Damage in Organic Crystals. I. $CH(COOH)_2$ in Malonic Acid[1]

By H. M. McConnell,[2] C. Heller,[3] T. Cole and R. W. Fessenden[4]

Received June 18, 1959

An analysis of the electron magnetic resonance of single crystals of malonic acid that were subjected to X-ray damage indicates that: (a) the principal long-lived paramagnetic species produced by the X-ray damage is $CH(COOH)_2$. (b) The carbon, oxygen and carboxyl hydrogen atoms of this radical are oriented in the crystalline lattice in the same way as these atoms are arranged in the parent undamaged malonic acid molecule. (c) The z,x,y components of the diagonal (electron-spin)-(nuclear-spin) coupling dyadic for the proton attached to the α-carbon atom are found to be of the same relative sign and of magnitudes 29, 61 and 91 Mc., respectively. In this orthogonal axis system, z is the CH bond direction and x is perpendicular to the plane of the three carbon atoms. These results are in excellent agreement with theoretical values of the distributed dipole and contact hyperfine interactions and show that this molecule is a π-electron radical, that the unpaired electron is concentrated almost entirely on the α-carbon and that the spin density on the in-plane σ-proton is negative. The observed g-factors for this radical are $g_x = 2.0026$, $g_y = 2.0035$ and $g_z = 2.0033$ and are in good qualitative agreement with previous theoretical estimates of these quantities.

Introduction

The electron magnetic resonance spectra of a large number of organic radicals have now been observed. The recent book by Ingram summarizes much of this work through the first part of 1958.[6] These electron magnetic resonance spectra have been used to identify radicals and to obtain information on their geometrical and electronic structures. The observed spectra of organic radicals may be divided rather sharply into two groups. In the first group are spectra obtained under conditions where the radicals undergo rapid isotropic tumbling motions. This is usually the situation when the radical is in a liquid solution of low viscosity, but comparatively free tumbling motions are also known for radicals trapped in "rigid" matrices at low temperatures.[7,8] Proton hyperfine splittings in the electron magnetic resonance of these systems arise from the isotropic Fermi contact interaction.[9] In strong fields of 3,000–10,000 gauss these spectra are usually quite sharp and are easily interpreted in terms of isotropic coupling constants. The relative intensities of the various signals in a hyperfine multiplet, and the magnitudes of the isotropic coupling constants can be interpreted in terms of the geometrical and electronic structures of the radicals.

In the second group are placed the spectra of organic radicals whose orientations are fixed in a solid solution or crystalline lattice. Proton hyperfine splittings in the spectra of these radicals arise from the combined effects of the isotropic Fermi contact interaction, and the anisotropic (electron-spin)-(nuclear-spin) dipolar interaction. These two magnetic interactions are of the same magnitude.[10] The interpretation of resonance spectra with anistropic contributions may be quite involved but is potentially rewarding in terms of the additional information on molecular structure that can be deduced from observed anisotropic interactions. Unfortunately, the spectra of polycrystalline samples, or the spectra of radicals randomly trapped in solid solution in a rigid glass, yield comparatively little information on the hyperfine interactions since, because of the anistropy, the resonance lines are generally broad, and the weaker resonance signals are often obscured by the broad intense signals.

In these laboratories it has been observed that (a) paramagnetic radicals are produced in a large number of organic single crystals when damaged by exposure to X-rays, and (b) these radicals have well-defined orientations in the crystal lattice. Many of the radicals are stable in the crystalline lattice at room temperature. Such systems are then ideally suited to an investigation of the anisotropy of the hyperfine spectra. It is planned that this paper will be the first of a series dealing with the interpretation of anisotropic proton hyperfine interactions in the resonance spectra of radiation damaged organic crystals. A preliminary report on the subject matter of the present paper has already been published.[11]

Although there is already a massive literature on the paramagnetic resonance spectra of organic radicals produced by radiation damage in solids and glasses, there are relatively few published analyses of proton anisotropic hyperfine structure. Whiffen[12] has made an analysis of this type for X-ray irradiated single crystals of glycine, with experimental results similar to those obtained in the present work with malonic acid. Also, Miyagawa and Gordy[13] have made a study of the anisotropic magnetic resonance of γ-irradiated single crystals of alanine.

Experimental

Single crystals of malonic acid were grown by the slow evaporation of aqueous solutions. The crystals had well-developed faces and were several millimeters in length on

(1) Spousored by the Office of Ordnance Research, U. S. Army, by the Office of Naval Research under project NR051-248, by the National Science Foundation, and by the United States Public Health Service.

(2) Alfred P. Sloan Fellow.

(3) A. A. Noyes Postdoctoral Fellow.

(4) National Science Foundation Postdoctoral Fellow.

(5) Contribution No. 2472.

(6) D. J. E. Ingram, "Free Radicals as Studied by Electron-Spin Resonance," Butterworth Scientific Publications, London, 1958.

(7) H. M. McConnell, *J. Chem. Phys.*, **29**, 1422 (1958); S. N. Foner, E. L. Cochran, V. A. Bowers and C. K. Jen, *Phys. Rev. Letters*, **1**, 91 (1958).

(8) T. Cole, H. O. Pritchard, N. R. Davidsou and H. M. McConnell, *Molecular Physics*, **1**, 406 (1958).

(9) S. I. Weissman, *J. Chem. Phys.*, **22**, 1378 (1954).

(10) H. M. McConnell and J. Strathdee, *Molecular Physics*, **2**, 129 (1959).

(11) T. Cole, C. Heller and H. M. McConnell, *Proc. Natl. Acad. Sci., U. S.*, **45**, 525 (1959).

(12) D. K. Ghosh and D. H. Whiffen, *Molecular Physics*, **2**, 285 (1959).

(13) I. Miyagawa and W. Gordy, *Bull. Amer. Phys. Soc.*, **4**, 260 (1959); *J. Chem. Phys.*, **30**, 1590 (1959).

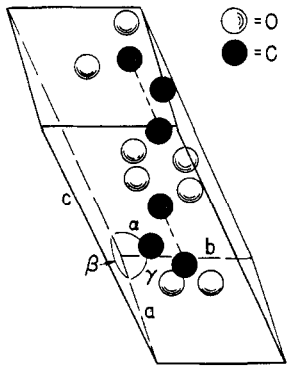

Fig. 1.—Sketch of the unit cell of malonic acid.

each side. Malonic acid is triclinic. The crystal structure has been determined by Goedkoop and MacGillavry.[14] A unit cell is sketched in Fig. 1. The unit cell edges are a = 5.33 Å., b = 5.14 Å., c = 11.25 Å., and the triclinic angles are α = 102° 42′, β = 135° 10′ and γ = 85° 10′. The unit cell contains two molecules that are related by a center of symmetry. The molecules are hydrogen bonded end-to-end, and form "infinite" chains parallel to the c-axis. The carboxyl group nearest the center of the unit cell is twisted 13° from the plane of the three carbon atoms. The other carboxyl group is twisted about 90°. The carbon atoms are approximately in the 210 plane.

The triclinic crystal axes were identified with an optical goniometer. It was found that three crystal edges intersected in a point with angles equal to the unit cell angles, α,β,γ, reported by Goedkoop and MacGillavry.[14] The unit cell axes a,b,c in Fig. 1 then were assumed to be parallel to these crystal edges.

A single crystal of malonic acid was subjected to X-rays from a tungsten target operating at 50 kv. and 30 ma. The distance of the crystal from the target was about 5 cm. The irradiation period varied from 30 to 45 minutes. The electron magnetic resonance spectra of single crystals were observed at X-band (9,500 Mc.) with a Varian Associates V-4, 500 Spectrometer and at K-band (24,100 Mc.) with a spectrometer of conventional design built in this Laboratory.

In general an irradiated single crystal showed a large number (up to fourteen) of resonance lines when examined immediately after irradiation. However, when an irradiated crystal was allowed to age at room temperature, the relative intensities of many of the lines decreased, and usually only two strong lines remained after a prolonged aging of about two months. The same effect also could be accomplished by warming a crystal to 50–60° for 24 hr. The study of these persistent resonance lines is the subject of the present paper. Unless indicated otherwise, our discussion of spectra shall always refer to aged, or heat-treated, single crystals. All the spectra reported in the present work were taken at room temperature.

At least one hundred spectra were observed. In each spectrum one can, with extremely few exceptions, divide the resonance signals into two classes, the "*strong*" and "*weak*" resonance signals. The *strong* signals were at least 5–10 times more intense than the *weak* signals. In most spectra there are only two *strong* signals; in some there are four. As we shall show later, *all of the intense signals are due to the radical* $CH(COOH)_2$, *some of the weak signals are due to the radical* $CH(COOH)_2$, *and some of the weak signals are thought to be due to one or more unidentified radical species present in relatively low concentration.* For example, the outermost *weak* signals in the X-band resonances in Figs. 2 and 3 are thought to be due to a second radical species since (a) these outermost signals are the most intense when the crystal is irradiated and studied at liquid nitrogen temperature, and (b) the g-values for these outermost signals are somewhat different from those of the strong signals at some orientations. Also, these outermost signals microwave power saturate much less easily.

The other important example of *weak* signals that we ascribe to one or more additional radical species is illustrated in Fig. 2b. In this spectrum *all* of the *weak* signals are attributed to secondary molecular species. This conclusion is also suggested by the fact that when the crystal is irradiated and studied at liquid nitrogen temperatures, the spectrum shows a very intense and broad resonance at a field position corresponding to the center of the spectrum in Fig. 2b.

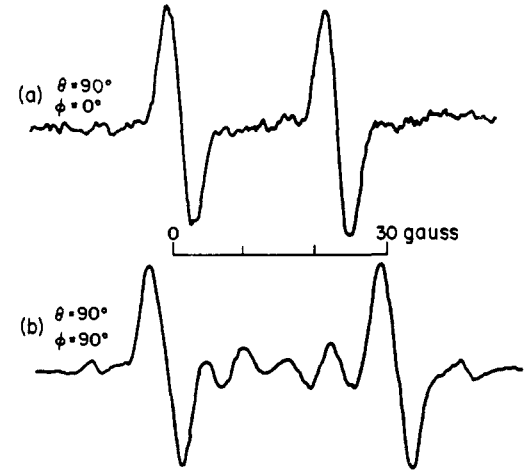

Fig. 2.—X-Band electron magnetic resonance of an irradiated single crystal of malonic acid with the applied field in (a) the x-direction, and (b) the y-direction.

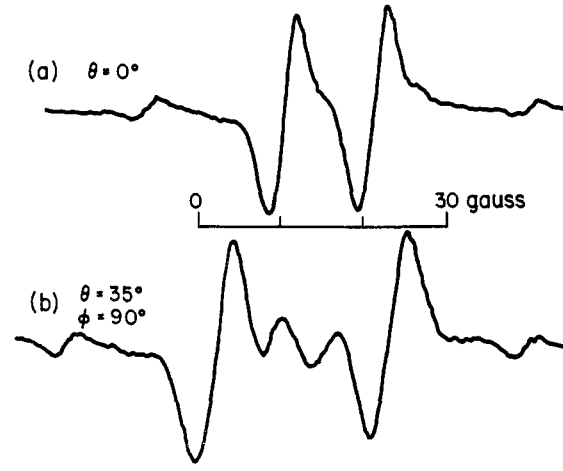

Fig. 3.—X-Band electron magnetic resonance of an irradiated single crystal of malonic acid with the applied field in (a) the z-direction, and (b) the z-y quadrant, where ϑ = 35°, φ = 90°.

On the other hand, for example, the two *weak* signals between the two strong signals in Fig. 3b, and the two *weak* outer signals in Fig. 5b are predicted by theory to be due to the radical $CH(COOH)_2$.

For the X-band resonance work a small Teflon goniometer head was constructed which permitted the rotation of an irradiated single crystal about two orthogonal axes within an X-band microwave cavity. The crystal was cemented to the mounting with wax, and crystal positioning was made by eye with the aid of a binocular microscope. K-band spectra at different orientations were obtained with the aid of a rotating magnet. Illustrative X-band spectra are given in Figs. 2 and 3, and K-band spectra are given in Figs. 4–6. The polar and azimuthal angles, ϑ and φ in these figures give the orientation of the applied magnetic field relative to an x, y, z Cartesian axis system fixed in the crystal. This axis system is defined as follows. The z-axis lies in the plane of the three carbon atoms and bisects the H–C–H angle in the CH_2 groups of malonic acid. The x-axis is perpendicular to the plane of the three carbon atoms. The y-axis is the third axis of an orthogonal right-handed system. For con-

(14) J. A. Goedkoop and C. H. MacGillavry, *Acta Cryst.*, **10**, 125 (1957).

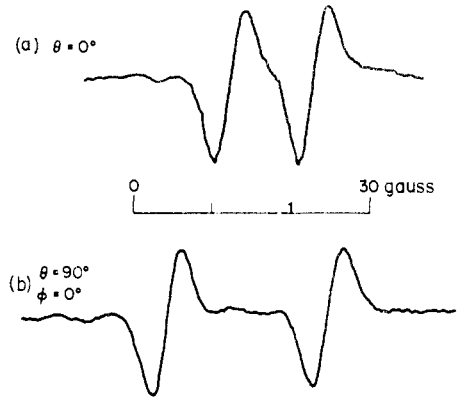

Fig. 4.—K-Band electron magnetic resonance of an irradiated single crystal of malonic acid with the applied field in (a) the z-direction, and (b) the x-direction.

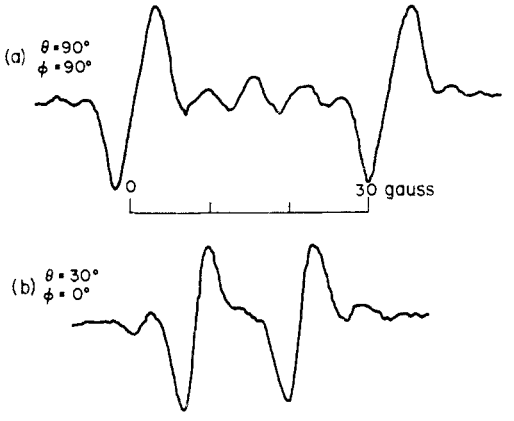

Fig. 5.—K-Band electron magnetic resonance of an irradiated single crystal of malonic acid with the applied field in (a) the y-direction, and (b) the z-x quadrant, with $\vartheta = 30°$, $\varphi = 0°$.

venience the origin of this axis system is placed at the carbon atom of a CH_2 group. The polar angle ϑ gives the angle between the field direction and the z-axis, and $\sin\vartheta\cos\varphi$ is the projection of the field direction along the x-axis.

The N^{14} splittings of the three lines of peroxylamine disulfonate in aqueous solution were used for calibration purposes.[15] Spectroscopic splitting factors were measured in the x, y and z directions using this inorganic radical. The splitting factors are designated g_x, g_y and g_z, respectively. The experiments were carried out by placing both the malonic acid crystal and a solution of peroxylamine disulfonate in an X-band microwave cavity. The results are $g_x = 2.0026$, $g_y = 2.0035$ and $g_z = 2.0033$. The absolute values of any one of the g-factors is uncertain to ± 0.0004 while the relative values are accurate to within ± 0.0001.

The Spin Hamiltonian

The spin Hamiltonian that can be used to interpret the electron magnetic resonance spectra of oriented radicals is

$$\mathcal{H} = \mathcal{H}_z + \mathcal{H}_{hf} \qquad (1)$$

Here $\mathcal{H}_z$ is the Zeeman coupling of the electronic and nuclear magnetic moments, μ_e and μ_n, to the externally applied field $\mathbf{H}_0$.

$$\mathcal{H}_z = -\boldsymbol{\mu}_e\cdot\mathbf{H}_0 - \boldsymbol{\mu}_n\cdot\mathbf{H}_0 \qquad (2)$$

Let us consider a radical containing only a single proton; in this case equation 2 may be written

$$\mathcal{H}_z = |\beta|\,\mathbf{S}\cdot\mathbf{g}\cdot\mathbf{H}_0 - \beta_N g_N \mathbf{I}_H \qquad (3)$$

In equation 3, $|\beta|$ is the absolute value of the electronic Bohr magneton, β_N is the nuclear Bohr magneton, $\mathbf{g}$ is the spectroscopic splitting factor dyadic and g_N is the nuclear g-factor. $\mathbf{I}_H$ is the component of the nuclear spin angular momentum in the field direction, in units of $\hbar$. For most organic radicals, the $\mathbf{g}$ dyadic is almost equal to g_0 times the unit dyadic (idemfactor), where g_0 is the "free-spin" g-factor, $g_0 = 2.0023$. We shall usually assume this to be so in the present paper; in this case equation 3 may be written in the more convenient form

$$\mathcal{H}_z = h|\nu_e|\mathbf{S}_H - h\nu_p\mathbf{I}_H \qquad (4)$$

where the electron and nuclear resonance frequencies $|\nu_e|$ and ν_p are

$$|\nu_e| = h^{-1} g_0|\beta|H_0 \qquad (5)$$

$$\nu_p = h^{-1} g_N\beta_N H_0 \qquad (6)$$

In the present work $|\nu_e| = 9{,}500$ Mc. and $\nu_p = 14.5$ Mc. for X-band and $|\nu_e| = 24{,}100$ Mc. and $\nu_p = 36.6$ Mc. at K-band.

The (electron-spin)-(nuclear-spin) hyperfine interaction Hamiltonian is

$$\mathcal{H}_{hf} = \mathbf{S}\cdot\mathbb{S}\cdot\mathbf{I} + \mathbf{V}\cdot(\mathbf{S}\times\mathbf{I}) \qquad (7)$$

Equation 7 includes the combined (electron-spin)-(nuclear-spin) Fermic contact interaction, the (electron-spin)-(nuclear-spin) dipolar interaction and the (electron-orbit)-(nuclear-spin) and (electron-spin)-(electron-orbit) magnetic interactions. We assume the absence of orbital degeneracy. In equation 7 $\mathbb{S}$ is a symmetric dyadic, and $\mathbf{V}$ is a pseudovector fixed in the radical.[16,17] The pseudovector hyperfine interaction occurs when the axes of the diagonalized $\mathbf{g}$ dyadic cannot be made parallel to the diagonalized (electron-spin)-(nuclear-spin) dipolar interaction.[16,17] It can be shown[16] that the pseudovector interaction is of the order of Δg times the dipolar interaction, where Δg is a typical anisotropy in $\mathbf{g}$. In the present work

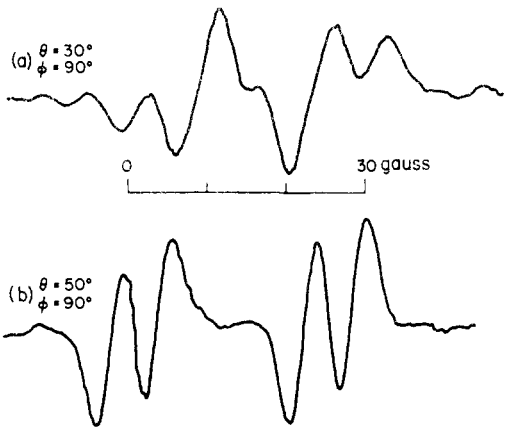

Fig. 6.—K-Band electron magnetic resonance of an irradiated single crystal of malonic acid with the applied field in (a) the z-y quadrant with $\vartheta = 30°$, $\varphi = 90°$ and (b) the z-y quadrant with $\vartheta = 50°$ and $\varphi = 90°$.

(15) G. E. Pake, J. Townsend and S. I. Weissman, *Phys. Rev.*, **85**, 682 (1952).

(16) H. M. McConnell, *Proc. Natl. Acad. Sci. U. S.*, **44**, 766 (1958).

(17) H. M. McConnell and R. E. Robertson, *J. Chem. Phys.*, **29**, 1361 (1958).

the Δg's have been measured and are of the order of 10^{-8} or less. Thus, the pseudovector interaction is of the order of 10^{-3} smaller than the dipolar component of $\mathcal{S}$ in equation 7 and is completely negligible in the present problem. Thus, we only include the symmetric dyadic in equation 7 and write this in the diagonal form

$$\mathcal{H}_{hf} = hA\mathbf{S}_{x'}\mathbf{I}_{x'} + hB\mathbf{S}_{x'}\mathbf{I}_{x'} + hC\mathbf{S}_{y'}\mathbf{I}_{y} \quad (8)$$

In equation 8, x', y', z' is a set of Cartesian axes for which $\mathcal{S}$ is diagonal.

In molecules with negligible spin–orbit interaction, the anisotropic components of $\mathcal{S}$ arise from (electron-spin)–(nuclear-spin) dipolar interactions, and the isotropic components arise from the Fermi contact interaction. Thus

$$\begin{aligned} A &= A_d + a \\ B &= B_d + a \\ C &= C_d + a \end{aligned} \quad (9)$$

Here a is the isotropic interaction, and A_d, B_d, and C_d are the dipolar contributions to A, B, C. The trace of the dipolar contribution to $\mathcal{S}$ is zero.

$$A_d + B_d + C_d = 0 \quad (10)$$

These hyperfine interactions are then simply related to the distribution of electron spin angular momentum in the paramagnetic molecule. Let $\hbar\mathbf{S}\rho(\mathbf{r})$ be the vector density of electron-spin angular momentum at the position $\mathbf{r}$ in a molecule. The scalar quantity $\rho(\mathbf{r})$ is called the spin density distribution function.[18] If $\mathbf{r}_N$ is the vector position of the proton, then the isotropic coupling constant a is[18–20]

$$a = h^{-1}g_0|\beta|g_N\beta_N\frac{8\pi}{3}\rho(\mathbf{r}_N) \quad (11)$$

The principal components of the dipolar interaction are[10]

$$A_d = -h^{-1}g_0|\beta|g_N\beta_N\int_\epsilon \rho(\mathbf{r})\frac{(1 - 3\cos^2\vartheta')}{|\mathbf{r} - \mathbf{r}_N|^3}\,dV \quad (12)$$

$$B_d = -h^{-1}g_0|\beta|g_N\beta_N\int_\epsilon \rho(\mathbf{r})\frac{(1 - 3\sin^2\vartheta'\cos^2\varphi')}{|\mathbf{r} - \mathbf{r}_N|^3}\,dV \quad (13)$$

$$C_d = -h^{-1}g_0|\beta|g_N\beta_N\int_\epsilon \rho(\mathbf{r})\frac{(1 - 3\sin^2\vartheta'\sin^2\varphi')}{|\mathbf{r} - \mathbf{r}_N|^3}\,dV \quad (14)$$

In equations 12–14, ϑ' and φ' are the polar and azimuthal angles of the vector $\mathbf{r} - \mathbf{r}_N$ in the x',y',z'-axis system. The symbol ϵ indicates that a small region about the nucleus with volume of the order of $(\hbar/mc.)^3$ is omitted from the integrations. This omission is of no practical importance in our calculations here. We shall later consider the relation of the spin-density distribution to the electronic structure of the paramagnetic radical.

Analysis of the Spectra

Although it is generally possible to *fit* electron magnetic resonance spectra to a spin Hamiltonian without a detailed knowledge of the paramagnetic molecule giving the resonance, our present discussion is greatly simplified by using a specific molecular model for interpreting the spectra. This model is described by the set of assumptions (a) – (d) given below. These assumptions are then justified, first by showing that they can account for the observed anisotropy of the hyperfine structure of all *strong* resonance lines at all crystal orientations. The assumptions are further justified by showing that the anisotropy of the *strong* lines requires the simultaneous presence in the spectrum of *weak* lines at certain crystal orientations and that when these *weak* lines are predicted to have observable intensity, they are always found. We do not account for the presence of *all weak* lines since some of these almost certainly come from other radical species, as discussed in the experimental section. Finally, the assumptions given below are still further justified by showing that the parameters of the spin Hamiltonian deduced on the basis of these assumptions are just exactly equal to those expected from electronic structure theory.

(a) The *strong* resonance signals illustrated in Figs. 2–6 are due to radicals with the formula $CH(COOH)_2$.

(b) The carbon, oxygen and carboxyl hydrogen atoms have very nearly the same positions in the unit cell as they did in the parent $CH_2(COOH)_2$ molecules. In $CH(COOH)_2$ the α-proton is coplanar with the three carbon atoms, and the CH bond bisects the H–C–H angle of the undamaged parent malonic acid molecule. Thus, the CH bond is along the z-axis of the x,y,z-Cartesian axis system used above in discussing the spectra in Figs. 2–6.

(c) The x',y',z'-axis system that diagonalizes the hyperfine interaction (*cf.* equation 8) coincides with the x,y,z-axis system: $x = x'$, $y = y'$ and $z = z'$. The radical x,y,z-axis system is illustrated in Fig. 7.

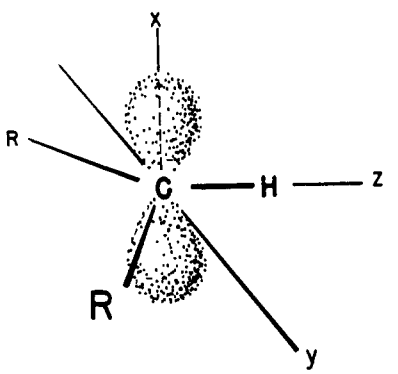

Fig. 7.—The x,y,z Cartesian axis system: this axis system is defined in the Experimental section in terms of the crystal orientation of an undamaged malonic acid molecule. This figure illustrates the position of the radical $CH(COOH)_2$ in this x,y,z axis system according to assumptions (b) and (c) in the section on analysis of spectra; R = COOH. The dotted area represents the unpaired spin distribution of a single π-electron localized in a $2p_x$ atomic orbital centered on the carbon atom at the origin of coördinates in this figure.

(d) The only significant hyperfine interaction is between the α-proton and the electronic-spin angular momentum.

According to assumptions (a) and (b), all of the $CH(COOH)_2$ molecules either have identical orientations in space or are related to one another

(18) H. M. McConnell, *J. Chem. Phys.*, **28**, 1188 (1958).
(19) E. Fermi, *Z. Physik*, **60**, 320 (1930).
(20) H. M. McConnell and D. B. Chesnut, *J. Chem. Phys.*, **28**, 107 (1958).

by a center of symmetry. Thus, all $CH(COOH)_2$ molecules must give identical spectra. In interpreting the spectra, we then shall consider only one molecule.[21] (As we shall see later, this interpretation is indeed possible, showing that all radicals giving *strong* lines do indeed have identical orientations in the crystal lattice or are related by a center of symmetry. This, of course, supports the validity of assumptions (a) and (b).)

Under assumptions (a)–(d), three orientations of crystal in the magnetic field give particularly simple spectra. These three *canonical orientations* correspond to the applied field direction along the x, y or z-axes. The eigenvalues of the Hamiltonian in equation 1 can be obtained by inspection for the three canonical orientations. For the z-canonical orientations ($\mathbf{H}_0$ along the z-axis), the electron resonance is a simple doublet with splitting equal to $|A|$. Similarly, the x- and y- canonical orientations give simple doublets with splittings equal to $|B|$ and $|C|$, respectively. For these canonical orientations the hyperfine spacings do not depend on the applied field strength, as long as $|\nu_e| >> |A|, |B|, |C|$. In our experimental work, we first oriented the crystal along the molecular y-axis, which is closely parallel to the crystal c-axis.[14] The observed X-band spectrum is given in Fig. 2b. The doublet splitting is 91 Mc., which is the absolute value of C. This is

$$|C| = 91 \pm 2 \text{ Mc.} \qquad (15)$$

the largest splitting that is observed at any crystal orientation. The *weak* lines in Fig. 2b are attributed to a second radical species. The K-band resonance spectrum for the y-canonical orientation is given in Fig. 5a. At this frequency the observed splitting was 90 ± 2 Mc. This agreement indicates that the y-direction is indeed a canonical direction; this result supports assumption (c) above to the extent that $y = y'$. Note that in general in the intermediate field region where this work is carried out, splittings between *strong* resonance lines usually depend strongly on the field strength for a general crystal orientation.

The X-band resonance spectrum in the z-canonical orientation is given in Fig. 3a. This orientation was obtained by orienting a crystal so that the magnetic field was perpendicular to the crystalline c-axis and in the 210 plane. This orientation of the crystal was made by eye, sometimes using a binocular microscope. According to assumption c, the doublet splitting in Fig. 3a is the absolute value of A

$$|A| = 29 \pm 2 \text{ Mc.} \qquad (16)$$

This splitting of the *strong* doublet is the smallest splitting that could be observed at any crystal orientation. The K-band resonance for the z-canonical orientation is given in Fig. 4a. The observed splitting is 29.5 ± 2 Mc. and is in good agreement with the splitting at X-band, thus supporting assumption c with respect to the equality of z and z'. If $y = y'$ and $z = z'$, then it follows that $x = x'$. Of course, these results only establish assumptions c to within the experimental error, which is roughly $\leqslant \pm 3°$ for the y-canonical orientation, and $\leqslant \pm 5°$ for the z-canonical orientation.

The X-band resonance doublet for the x-canonical orientation is given in Fig. 2a. This orientation was obtained by applying the steady magnetic field so that it was perpendicular to the previously identified y- and z-axes. This splitting gives the absolute value of B. The K-band doublet for the x-canonical orientation is given in Fig. 4b and is equal to 58 ± 2 Mc.

$$|B| = 61 \pm 2 \text{ Mc.} \qquad (17)$$

With a suitable choice of relative signs, the above values of A, B and C must then account for all spectra at other crystal orientations. The calculation of the resonance spectra for a general orientation is not entirely trivial. We therefore give below an outline of a particularly convenient procedure for making this calculation and a set of theorems that permit a rapid interpretation of the important qualitative features of observed spectra.

When $|\nu_e|, >> |A|, |B|, |C|$ one may neglect the vector components of $\mathbf{S}$ that are perpendicular to $\mathbf{H}_0$. The eigenvalues of the total spin Hamiltonian may be written in the particularly simple form

$$E = h|\nu_e|S_H - h\nu I_u \qquad (18)$$

where S_H is one of the eigenvalues ($\pm 1/2$) of the operator $\mathbf{S}_H$, and I_u is one of the eigenvalues ($\pm 1/2$) of the operator $\mathbf{I}_u$ for the component of the nuclear spin angular momentum in the direction of the unit vector $\mathbf{u}$. The frequency ν represents the resonance frequency of the proton in the net magnetic field (applied plus hyperfine) acting at the position of the proton. The unit vector $\mathbf{u}$ gives the direction of this net field. Both ν and $\mathbf{u}$ depend on the eigenvalue S_H, as indicated in the equation

$$\nu\mathbf{u} = \nu_p\mathbf{u}_H - S_H[\mathbf{k}A\cos\vartheta + \mathbf{i}B\sin\vartheta\cos\varphi + \mathbf{j}C\sin\vartheta\sin\varphi] \qquad (19)$$

In equation 19, $\mathbf{i}$, $\mathbf{j}$, $\mathbf{k}$ are unit vectors in the direction of the positive x,y,z-axes, respectively. Note that in this equation the direction of the vector $\mathbf{u}$ is defined by the direction of the vector on the right-hand side of this equation, and the frequency ν is the length of this vector. Note also that ν is defined so that it is a *positive* quantity. In the following discussion it will be convenient to adopt the convention that we use a single prime to denote spin eigenstates for which the eigenvalue S_H is $1/2$, and a double prime to denote spin eigenstates for which this eigenvalue is $-1/2$. Thus, $S_H' = 1/2$, $S_H'' = -1/2$. Correspondingly, there are two groups of eigenenergies E' and E'', two frequencies ν' and ν'', and two unit vectors $\mathbf{u}'$ and $\mathbf{u}''$. A subscript equal to 1 indicates the component of nuclear spin to be $1/2$, and a subscript equal to 2 indicates the component of nuclear spin is $-1/2$. Thus

$$E_1' = 1/2h|\nu_e| - 1/2h\nu' \qquad (20)$$

$$E_2' = 1/2h|\nu_e| + 1/2h\nu' \qquad (21)$$

$$E_1'' = -1/2h|\nu_e| - 1/2h\nu' \qquad (22)$$

(21) In unpublished work on several radiation damaged organic crystals having a variety of crystal structures, it has been found that the anisotropic hyperfine structure in the resonance spectra shows the point group symmetry of the undamaged crystal, and this implies that the radicals are related to one another by the space group symmetry operations of the crystal.

$$E_2'' = -\tfrac{1}{2}h|\nu_e| + \tfrac{1}{2}h\nu'' \quad (23)$$

The corresponding spin eigenfunctions are

$$\psi_1' = \alpha(e)\alpha'(p) \quad (24)$$
$$\psi_2' = \alpha(e)\beta'(p) \quad (25)$$
$$\psi_1'' = \beta(e)\alpha''(p) \quad (26)$$
$$\psi_2'' = \beta(e)\beta''(p) \quad (27)$$

The spin functions are defined by the equations

$$\mathbf{S}_H\alpha(e) = S_H'\alpha(e) \quad (28)$$
$$\mathbf{S}_H\beta(e) = S_H''\beta(e) \quad (29)$$
$$\mathbf{I}_u'\alpha'(p) = \tfrac{1}{2}\alpha'(p) \quad (30)$$
$$\mathbf{I}_u'\beta'(p) = -\tfrac{1}{2}\beta'(p) \quad (31)$$
$$\mathbf{I}_u''\alpha''(p) = \tfrac{1}{2}\alpha''(p) \quad (32)$$
$$\mathbf{I}_u''\beta''(p) = -\tfrac{1}{2}\beta''(p) \quad (33)$$

The electron resonance transition frequencies are

$$(E_1' - E_1'')h^{-1} = |\nu_e| - \tfrac{1}{2}(\nu' - \nu'') \quad (34)$$
$$(E_2' - E_2'')h^{-1} = |\nu_e| + \tfrac{1}{2}(\nu' - \nu'') \quad (35)$$
$$(E_1' - E_2'')h^{-1} = |\nu_e| - \tfrac{1}{2}(\nu' + \nu'') \quad (36)$$
$$(E_2' - E_1'')h^{-1} = |\nu_e| + \tfrac{1}{2}(\nu' + \nu'') \quad (37)$$

The electron resonance transition probabilities are proportional to the absolute square matrix elements given below, where $\mathbf{S}_\perp$ is the operator for a component of $\mathbf{S}$ perpendicular to $\mathbf{H}_0$.

$$|(\psi_1'|\mathbf{S}_\perp|\psi_1'')|^2 = \tfrac{1}{4}|(\alpha'(p)|\alpha''(p))|^2 \quad (38)$$
$$|(\psi_2'|\mathbf{S}_\perp|\psi_2'')|^2 = \tfrac{1}{4}|(\beta'(p)|\beta''(p))|^2 \quad (39)$$
$$|(\psi_1'|\mathbf{S}_\perp|\psi_2'')|^2 = \tfrac{1}{4}|(\alpha'(p)|\beta''(p))|^2 \quad (40)$$
$$|(\psi_2'|\mathbf{S}_\perp|\psi_1'')|^2 = \tfrac{1}{4}|(\beta'(p)|\alpha''(p))|^2 \quad (41)$$

The proton spin matrix elements are readily evaluated[22] in terms of the angle ξ between the vectors $\mathbf{u}'$ and $\mathbf{u}''$.

$$\mathbf{u}' \cdot \mathbf{u}'' = \cos\xi \quad (42)$$
$$|(\alpha'(p)|\alpha''(p))|^2 = |(\beta'(p)|\beta''(p))|^2 = \cos^2(\xi/2) \quad (43)$$
$$|(\alpha'(p)|\beta''(p))|^2 = |(\beta'(p)|\alpha''(p))|^2 = \sin^2(\xi/2) \quad (44)$$

In general, therefore, the resonance spectrum is a symmetrical quartet, centered on $|\nu_e|$. The outer doublet with splitting $(\nu' + \nu'')$ has relative intensity $\sin^2(\xi/2)$. The inner doublet with splitting $(\nu' - \nu'')$ has relative intensity $\cos^2(\xi/2)$.

We give below five general theorems that show a number of important qualitative features of this magnetic resonance quartet. These theorems are all valid when $|\nu_e| >> |A|, |B|, |C|$.

Theorem I. *The second-moment of the resonance quartet does not depend on the applied field strength.* The second-moment of the resonance quartet is defined by the equation

$$\langle(\Delta\nu)^2\rangle_{Av} = R_0(\nu' + \nu'')^2 + R_i(\nu' - \nu'')^2 \quad (45)$$

where R_0 is the relative intensity of the outer doublet and R_i is the relative intensity of the inner doublet. $R_0 = \sin^2(\xi/2)$; $R_i = \cos^2(\xi/2)$. The moment equation (46) may be derived using methods similar to those employed in various nuclear resonance problems.[23]

$$\langle(\Delta\nu)^2\rangle_{Av} = A^2\cos^2\vartheta + B^2\sin^2\vartheta\cos^2\varphi + C^2\sin^2\vartheta\sin^2\varphi \quad (46)$$

(22) See, for example, E. M. Corson, "Perturbation Methods in the Quantum Mechanics of *n*-Electron Systems," Hafner Publishing Co., 1948, p. 118.

(23) J. H. Van Vleck, *Phys. Rev.*, **74**, 1168 (1948); W. Anderson and H. M. McConnell, *J. Chem. Phys.*, **26**, 1496 (1957).

Theorem II. *In a canonical orientation the allowed transitions give a resonance doublet with splitting equal to $|A|$ or $|B|$ or $|C|$. The forbidden transitions for the canonical orientation have splittings equal to $2\nu_p$ in each case.*

Theorem III. *The outer resonance doublet never "crosses" or coincides with the inner doublet.* To prove this theorem, note first that if the outer doublet coincides with the inner doublet, then $|\nu' + \nu''| = |\nu' - \nu''|$. This can only be true if $\nu' = 0$, or $\nu'' = 0$. From equation 19 we can obtain (47), a perfectly general expression for ν

$$\nu = [(\nu_p - S_H A)^2\cos^2\vartheta + (\nu_p - S_H B)^2\sin^2\vartheta\cos^2\varphi + (\nu_p - S_H C)^2\sin^2\vartheta\sin^2\varphi]^{1/2} \quad (47)$$

Equation 47 gives ν' when $S_H = S_H'$ and gives ν'' when $S_H = S_H''$. The expression in the brackets in equation 47 is the sum of three squares. Also $|A| \neq |B| \neq |C|$. Thus, in general, ν will never be zero; the only possible exception to this is a canonical orientation for which $2\nu_p = |A|$ or $|B|$ or $|C|$. This exceptional case is of no practical importance since, from Theorem I, one pair of the doublets has zero intensity.

Theorem IV. *The outer doublet is more intense than the inner doublet if the second-moment of the hyperfine multiplet is greater than the square of twice the proton resonance frequency, and vice versa.* This theorem follows from the equation

$$R_0 - R_i = \frac{1}{\nu'\nu''}\{\langle(\Delta\nu)^2\rangle_{Av} - (2\nu_p)^2\} \quad (48)$$

which can be derived from equations 45, 46 and 47. There are several important corollaries to this theorem.

Corollary (A).—Since the second moment $\langle(\Delta\nu)^2\rangle_{Av}$ is never smaller than the smallest value of the hyperfine couplings squared, *i.e.*, A^2, B^2 or C^2, the outer lines will always be the most intense if A^2, B^2 and $C^2 > (2\nu_p)^2$. Contrawise, the inner lines will always be the most intense if $(2\nu_p)^2 > A^2, B^2, C^2$.

Corollary (B).—If the direction of the applied magnetic field is passed through an arc so that $\langle(\Delta\nu)^2\rangle_{Av} > (2\nu_p)^2$ at some angles and $\langle(\Delta\nu_p)^2\rangle_{Av} < (2\nu_p)^2$ at other angles, then there will be one orientation at which all four hyperfine multiplet lines have the same intensity.

Theorem V.—*The two lines of the inner doublet can never cross or coincide unless one of the hyperfine coupling constants A, B, C has a sign that is different from the other two.* The splitting of the inner doublet is $|\nu' - \nu''|$; if this is zero, $\nu' = \nu''$. From equation 47 one can show that equation (49) must hold if $\nu' = \nu''$.

$$A\cos^2\vartheta + B\sin^2\vartheta\cos^2\varphi + C\sin^2\vartheta\sin^2\varphi = 0 \quad (49)$$

Clearly, equation 49 can hold only if one of the coupling constants has a sign that is opposite to the other two. Note that the crossing angles in equation 49 do not depend on the strength of the applied field.

Now let us consider the experimental spectra that were obtained at intermediate orientations. To simplify both the experimental measurements and the mathematical analysis, most of these spectra were obtained by moving the field direction through one quadrant between two canonical

orientations. That is, the field was moved through the z-x quadrant ($\varphi = 0$, $0 \leq \vartheta \leq 90°$) and through the z-y quadrant ($\varphi = 90°$, $0 \leq \vartheta \leq 90°$). No attempt was made to obtain extensive data in the x-y quadrant since all of the important data could be obtained more readily from spectra in the x-z and y-z quadrants.

An X-band spectrum at an intermediate orientation in the z-y quadrant is illustrated in Fig. 3b. In the X-band experiments, the proton resonance frequency ν_p is 14.5 Mc., and $2\nu_p < |A|$, $|B|$ and $|C|$. Thus, according to Theorem IV, the outer lines of the quartet are strongest in all the X-band spectra. Figure 8 (lower) shows observed X-band hyperfine splittings in the z-y quadrant as a function of ϑ. In the upper half of Fig. 8 are given X-band hyperfine splittings calculated using equation

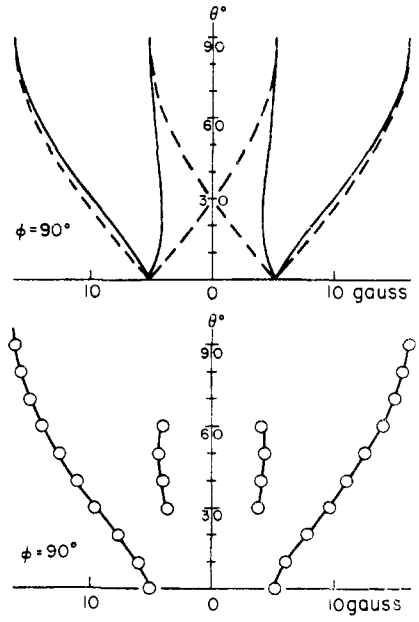

Fig. 8.—Calculated (upper) and observed (lower) X-band hyperfine splittings with the applied field in the z-y quadrant. In the upper diagram solid (dashed) lines give calculated resonance splittings with A and C of the same (opposite) sign.

47 (for ν' and ν'') and the values of $|A|$ and $|C|$ given in equation 16 and 17. The solid (and dashed) lines give calculated positions for A and C of the same (and opposite) relative sign. The observed splittings of the *strong* resonance signals follow closely the theoretically calculated splittings for *strong* outer doublet. The calculated resonance splittings agree somewhat better with the experimental results when A and C are of the same sign, but the dashed and solid lines in the upper half of Fig. 8 are so close that this particular result does not provide a critical test of the relative signs of A and C. The experimental inner doublet splittings given in the lower half of Fig. 8 arise from *weak* signals of the type appearing between the two *strong* signals illustrated in Fig. 3b. Note that the splittings of these *weak* signals are in good agreement with the calculated inner doublet splittings only when A and C are assumed to have the same relative sign. This identification of the *weak* inner doublet as belonging to $CH(COOH)_2$ is further substantiated by the fact that the observed (inner/outer) relative intensities (*e.g.*, $\sim 1/6$ in Fig. 3b) are in semi-quantitative accord with the calculated relative intensities ($\sim 1/9$ for $\vartheta = 35°$, $\varphi = 90°$) when A and C have the same sign. (If A and C are taken to have opposite signs, the calculated intensity ratios are (inner/outer) = 1/3.5.) These results do indicate that A and C have the same relative sign, but we cannot regard this as absolutely conclusive in view of the fact that other radical species also give *weak* signals in some of the spectra.

In Fig. 9 are given calculated (upper) and observed (lower) X-band hyperfine splittings for the applied field direction in the z-x quadrant. Here again the observed splittings for the *strong* outer

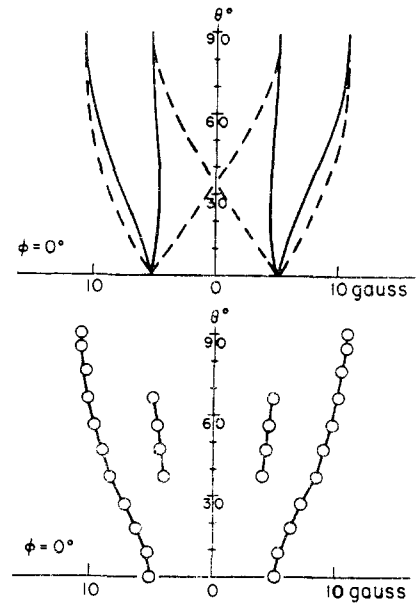

Fig. 9.—Calculated (upper) and observed (lower) X-band hyperfine splittings with the applied field in the z-x quadrant. In the upper diagram solid (dashed) lines give calculated resonance splittings with A and B of the same (opposite) sign.

lines are in good agreement with the calculated splittings, the agreement being better when A and B are taken to have the same relative sign. The observed splittings and relative intensities of the *weak* inner lines are also in good agreement with the calculated splittings and intensities only when A and B have the same relative sign. The calculated (inner/outer) relative intensities are here in the range $1/6 - 1/70$ for $35° \leq \vartheta \leq 70°$ when A and B are of the same sign.

We shall now show that the spectra at K-band frequencies further support our basic assumptions and provide a conclusive demonstration of the equality of the signs of A, B and C. Let us first consider the z-x quadrant. Without any detailed calculation we can see from our general theorems that spectra in the z-x quadrant must provide a critical test of the relative signs of A and B. From Theorem I we know that the second moment of the spectra in this quadrant can never exceed $|A|^2$ or $|B|^2$. That is, the second moment is never larger than $|B|^2$, or $\sim$(60 Mc.)^2 At K-band frequen-

cies $\nu_p = 36.6$, so that $(2\nu_p)^2 = (73.2 \text{ Mc.})^2$. From Theorem IV we know that the inner lines are more intense than the outer lines, and hence the inner lines must be *strong*. According to Theorem V, these *strong* inner lines will cross in the z-x quadrant if A and B have opposite signs; and, from equation 49, this crossing will occur at the polar angle ϑ that satisfies the equation

$$\tan\vartheta = \sqrt{-\frac{A}{B}} \simeq 1/\sqrt{2} \qquad (50)$$

That is, for $\vartheta \simeq 35°$. On the other hand, if A and B are of the same sign, then according to Theorem V the lines cannot cross. Thus, the crossing or non-crossing of the two *strong* resonance lines permits a clear-cut distribution to be made between the two possible relative signs of A and B. A K-band spectrum for this z-x quadrant is given in Fig. 5b for $\vartheta = 30°$, $\varphi = 0$. Figure 10 gives the observed (lower) and calculated (upper) K-band hyperfine splittings in this z-x quadrant. There is excellent agreement between observed and calculated splittings (and also relative intensities) only when A and B are of the same sign.

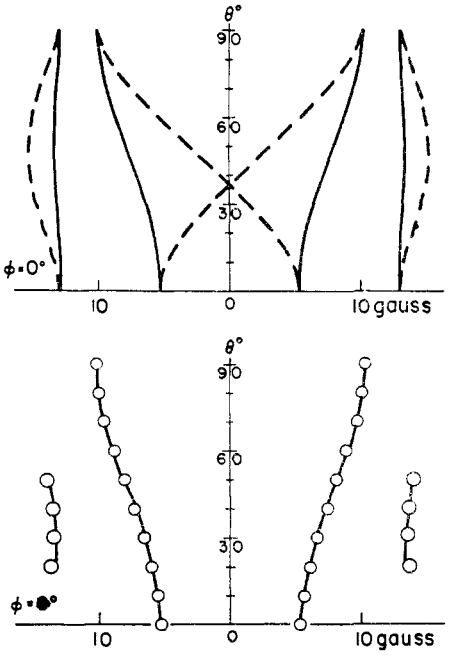

Fig. 10.—Calculated (upper) and observed (lower) K-band hyperfine splittings with the applied field in the z-x quadrant. In the upper diagram solid (dashed) lines give calculated resonance splittings with A and B of the same (opposite) sign.

Our general theorems show immediately that the K-band spectra in the z-y quadrant will be most unusual in that we must obtain *four strong lines of equal intensity at one orientation*. From Theorem I we see that the second moment in the z-y quadrant ranges between $|A|^2$ and $|C|^2$, that is, between $(29 \text{ Mc.})^2$ and $(90 \text{ Mc.})^2$. Since $(2\nu_p)^2 = (73.2)^2$, we see from Theorem IV that at some orientations in the z-y quadrant the outer lines are most intense, and at other orientations the inner lines are most intense. Therefore, there must be one orientation at which all four lines have equal intensity. An experimental spectrum illustrating this case is given in Fig. 6b. The question as to whether or not the spectra in this quadrant conclusively determine the relative signs of A and C depends on the intensity that the inner lines are calculated to have at the crossing angle. From Theorem V this crossing angle is calculated to be at $\sim 30°$. At this point the calculated (inner/outer) intensities are 3.5/1 for A and C of the same sign and 2/1 for A and C of opposite sign. Thus the crossing or non-crossing of *strong* lines can be used here to determine the relative signs of A and C. The K-band spectrum in Fig. 6a was taken in the z-y quadrant at $\vartheta = 30°$. The strong lines clearly do not coincide. Further, Fig. 11 gives observed (lower) and calculated (upper) K-band hyperfine splittings for the complete range of ϑ values in the z-y quadrant. Here there is good agreement between observed and calculated splittings at all orientations only when A and C have the same sign. Thus, A, B and C all have the same sign.

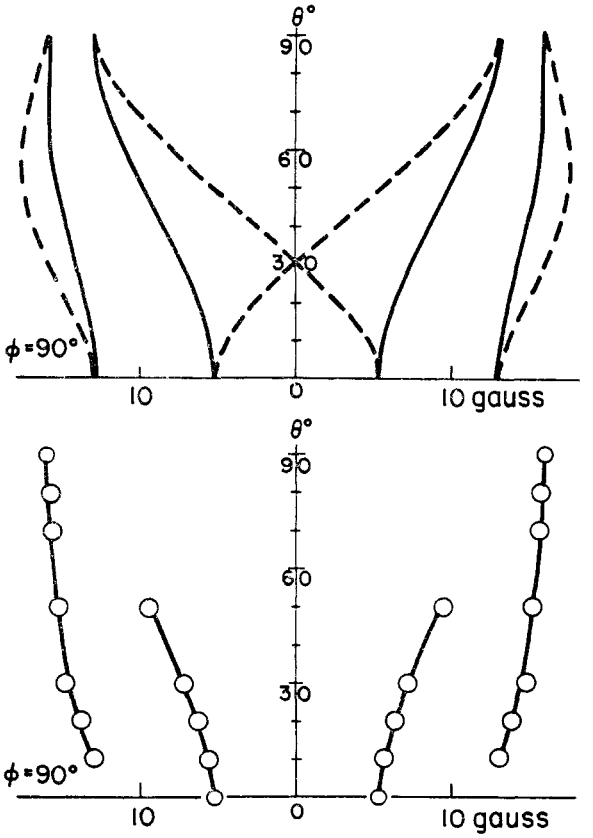

Fig. 11.—Calculated (upper) and observed (lower) K-band hyperfine splittings with the applied field in the z-y quadrant. In the upper diagram solid (dashed) lines give calculated resonance splittings with A and C of the same (opposite) sign.

We believe that the foregoing theoretical and experimental results strongly support assumptions (a) to (d) above, and that these assumptions are by far the most plausible that can be found that are compatible with the observed spectra.

Electronic Structure of $CH(COOH)_2$

Hyperfine Interactions.—In the present section we show that the observed hyperfine interactions in $CH(COOH)_2$ indicate that this molecule is a simple π-electron radical with essentially a unit odd-electron spin density on the central carbon atom. The radical is a π-electron radical in the sense that the odd electron spin is largely localized in an orbital antisymmetric to the plane containing three carbon atoms and the hydrogen atom. These conclusions are immediately suggested by the following argument.

In previous work it has been proposed,[24a] and shown on both theoretical[18,20,25] and experimental[26] grounds, that in π-electron radicals the isotropic proton hyperfine splitting for proton α, a_α, is proportional to the diagonal element of a π-electron-spin density matrix

$$a_\alpha = Q\rho^\pi_{\alpha\alpha} \qquad (51)$$

If we have only a single π-electron, as is the case in the present problem, then $\rho^\pi_{\alpha\alpha}$ is positive and is essentially the probability that the odd electron be found in the p_x orbital on the α-carbon atom. Experimental evidence from isotropic proton hyperfine splittings in the methyl radical[27-29] and the benzene negative ion[26b] indicate that $|Q| = 63$ Mc., while theoretical arguments[20,24] suggest that Q is negative, corresponding to a negative spin density at the proton when there is a positive spin density on the adjacent carbon atom. Since in the present work we have determined the relative signs of A, B and C for the α-proton in $CH(COOH)_2$, we may calculate the absolute value for the isotropic coupling from the equation

$$|a| = \frac{1}{3}|A + B + C| = 61 \pm 3 \text{ Mc.} \qquad (52)$$

This indicates that $CH(COOH)_2$ is indeed a π-electron radical with essentially a unit unpaired spin density on the α-carbon: $\rho^\pi_{\alpha\alpha} = 1$.

Let us now consider the anisotropic components of the observed hyperfine interaction. To do this it is convenient to expand the spin-density function $\rho(r)$ in terms of an atomic orbital spin-density matrix,[18] $\rho_{\lambda\mu}$

$$\rho(r) = \Sigma_{\lambda\mu}\rho_{\lambda\mu}\phi_\mu^*\phi_\lambda \qquad (53)$$

In equation 53, the set of numbers $\rho_{\lambda\mu}$ is called the atomic orbital spin-density matrix when the ϕ_μ and ϕ_λ are a complete set of one-electron atomic orbitals centered on various atoms. The expansion in equation 53 can be written as a sum of contributions from π-orbitals, and a sum of contributions from σ-orbitals, there being no cross terms.[10] For the present problem of the hyperfine interactions in $CH(COOH)_2$, we may write this expansion in terms of the orbitals

$$\rho(r) = \rho^\pi_{\alpha\alpha}\, p^2_x + \ldots\ldots + \rho^\sigma_{hh}(h_1^2 + h_2^2 + h_3^2) + \rho^\sigma_{ss}s^2 + \ldots\ldots \qquad (54)$$

In equations 54 the first set of dots indicates other π-orbitals that certainly make negligible contributions to the hyperfine structure; h_1 is a carbon sp^2 hybrid σ-orbital pointing from the carbon toward the proton, and h_2 and h_3 are the other two hybrid σ-orbitals that point from the α-carbon atom to the carboxyl carbon atoms. In equation 54 s is a 1s atomic orbital centered on the proton. The second set of dots in equation 54 indicates other σ-contributions that we have neglected. The anisotropic dipolar contributions to A, B and C are then obtained by substituting equation 54 in equations 12, 13 and 14 and carrying out the integrations. This has been done elsewhere[10] for the terms explicitly represented in equation 54 in the particular case that the $2p_x$, $2p_y$, $2p_z$, and $2s$ atomic orbitals of carbon are represented by Slater atomic orbitals with an effective nuclear charge equal to 3.18. In this work[10] the isotropic interaction was taken equal to -64 Mc. and the total (isotropic + anisotropic) theoretical coupling constants are

$$A_{\text{theo}} = -21\,(\rho^\pi_{\alpha\alpha} - 15.6\,\rho^\sigma_{hh}) \qquad (55)$$

$$B_{\text{theo}} = -69\,(\rho^\pi_{\alpha\alpha} + 2.7\,\rho^\sigma_{hh}) \qquad (56)$$

$$C_{\text{theo}} = -103\,(\rho^\pi_{\alpha\alpha} + 1.47\,\rho^\sigma_{hh}) \qquad (57)$$

Previous theoretical work[20] has indicated that $\rho^\sigma_{hh} \simeq -\rho^\sigma_{ss}$, and that $|\rho^\sigma_{ss}| = 0.1 - 0.01$. The known isotropic splitting in atomic hydrogen (1420 Mc.) suggests that $|\rho^\sigma_{ss}|$ of the order $(63/1420) \sim 0.04$, but more elaborate considerations[30] suggest that this over estimates $|\rho^\sigma_{ss}|$. Since we have found that $\rho^\pi_{\alpha\alpha} \simeq 1$, our theoretical estimates of B and C are not appreciably affected by uncertainties in ρ^σ_{hh}. It is quite plausible that the σ-anisotropic contribution to A is also negligible. Thus, the theoretical estimates of A, B and C for $CH(COOH)_2$ are

$$A_{\text{theo}} = -21 \text{ Mc.} \qquad (58)$$

$$B_{\text{theo}} = -69 \text{ Mc.} \qquad (59)$$

$$C_{\text{theo}} = -103 \text{ Mc.} \qquad (60)$$

There is excellent agreement between these numbers and the experimental results in equations 15, 16 and 17. There is also perfect agreement between the theoretical and experimentally determined relative signs.

It will be noted that if one had used $+64$ Mc. instead of -64 Mc. in calculating the isotropic contributions in equations 58–60, one would have obtained $A_{\text{theo}} = +107$ Mc., $B_{\text{theo}} = +59$ Mc. and $C_{\text{theo}} = +18$ Mc., in complete qualitative as well as quantitative disagreement with the observed A and C coupling constants. The negative isotropic interaction demonstrates that the spin density on the hydrogen atom is negative, an effect predicted some time ago on the basis of elementary electronic structure theory.[20,24a] The basic idea is illustrated in Fig. 12. When the electronic spin angular momentum in the p_x orbital on the carbon atom has some particular polarization, say "up," then there is a small spin polarization in the hybrid σ-orbital h_1

(24) (a) H. M. McConnell, *J. Chem. Phys.*, **24**, 632 (1956). (b) M. Krauss and J. F. Wehner, *ibid.*, **29**, 1287 (1958).

(25) H. M. McConnell, *Proc. Natl. Acad. Sci.*, **43**, 721 (1957).

(26) (a) S. I. Weissman, *J. Chem. Phys.*, **25**, 890 (1956). (b) S. I. Weissman, T. Tuttle and E. deBoer, *J. Phys. Chem.*, **61**, 28 (1957) (c) E. deBoer, *J. Chem. Phys.*, **25**, 190 (1956). (d) F. C. Adam and S. I. Weissman, THIS JOURNAL, **80**, 2057 (1958).

(27) C. F. Luck and W. Gordy, *ibid.*, **78**, 3240 (1956); W. Gordy and C. G. McCormick, *ibid.*, **78**, 3243 (1956).

(28) B. Smaller and M. S. Matheson, *J. Chem. Phys.*, **28**, 1169 (1958).

(29) C. K. Jen, S. N. Foner, E. L. Cochran and V. A. Bowers, *Phys Rev.*, **112**, 1169 (1958).

(30) H. Sternlicht and H. M. McConnell, to be published.

directed toward the hydrogen atom that is also "up" according to Hund's rule for spin correlation in orthogonal atomic orbitals of atoms. The spin on the proton tends to be antiparallel to the spin of the carbon atom because of ordinary covalent exchange bonding, and thus the spin polarization on the hydrogen atom is opposite (or negative) to the principal spin polarization in the p_x carbon atomic orbital.

Spectroscopic Splitting Factors.—The measurements of the spectroscopic splitting factors are described in the Experimental section. The results are $g_x = 2.0026$, $g_y = 2.0035$ and $g_z = 2.0033$. The absolute value of any one g-factor is uncertain to ± 0.004 while the relative values are accurate to within ± 0.0001. In previous work[31] on the theory of g-factors for π-electron radicals, it has been pointed out that the deviation of the g-factors from the free electron value arises from spin-orbit interaction on the carbon atom combined with the virtual excitation of a σ-bonding electron to the π-orbital, and the virtual excitation of a π-electron to a σ^*-antibonding orbital. In the coördinate system of the present paper, this previous work indicated that the $\sigma \rightarrow \pi$ excitations increase g_y and g_z by $2\,\zeta/\Delta E_2$, and the $\pi \rightarrow \sigma^*$ excitations decrease g_y and g_z by $2\,\zeta/\Delta E_1$. Here $\zeta(= 28\text{ cm.}^{-1})$ is the spin-orbit interaction parameter of atomic carbon,[32] and

(31) H. M. McConnell and R. E. Robertson, *J. Phys. Chem.*, **61**, 1018 (1957).

(32) D. S. McClure, *J. Chem. Phys.*, **20**, 682 (1952); **17**, 905 (1949).

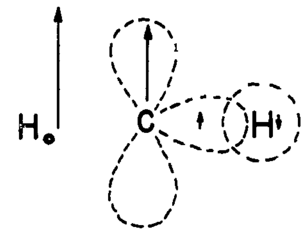

Fig. 12.—Spin polarizations on the α-carbon atom of $CH(COOH)_2$ and in the CH bond. The small spin density on the proton is negative (of opposite polarization) relative to the large π-electron spin density on the α-carbon atom.

ΔE_1 and ΔE_2 are the $\pi \rightarrow \sigma^*$ and $\sigma \rightarrow \pi$ one electron excitation energies, respectively. Excitations of the type $\sigma \rightarrow \sigma^*$ do not contribute appreciably to g_x-deviations since contributions from the six $\sigma \rightarrow \sigma^*$ excitations cancel if all three σ (sp^2 hybrid) bonds are equivalent. The large $\sigma \rightarrow \sigma^*$ excitation energy also diminishes this contribution. This previous work[31] suggested that the g_y and g_z values would be slightly *greater* than the free spin g-factor and that g_x would be close to the free spin g-value in π-electron radicals. The present experimental results are in accord with these ideas.

ADDED IN PROOF.—Zero-field resonance of $CH(COOH)_2$ has now been observed (H. M. McConnell, D. D. Thompson, and R. W. Fessenden, *Proc. Nat. Acad. Sci. U. S.*, **45**, 1600 (1959)). This work strongly supports the foregoing interpretation of the high field spectra.

Hyperfine splittings due to C^{13} in natural abundance in the central carbon atom have been observed (H. M. McConnell and R. W. Fessenden, *J. Chem. Phys.*, in press). This shows that the spin density in the hybrid orbital h_1 is positive, as illustrated in Fig. 12.

PASADENA, CALIFORNIA

[CONTRIBUTION FROM THE DEPARTMENT OF CHEMISTRY, UNIVERSITY OF ROCHESTER]

Photoisomerization of 5-Hexen-2-one[1]

BY R. SRINIVASAN

RECEIVED AUGUST 24, 1959

The photochemistry of 5-hexen-2-one has been studied in the vapor phase in the temperature range from 27 to 139° at 3130 Å. and also with radiation from an unfiltered mercury arc. The compound was found to be very stable toward photolysis. The most important product at 3130 Å. up to 139° was an isomer, the structure of which is most probably CH_3–C–O–CH_2–CH–CH_2–CH_2 (with ring bonds linking C to CH and C to the terminal CH_2). Evidence for this structure is based on the ultraviolet, infrared, nuclear magnetic resonance and mass spectra of the product. The quantum yield for the formation of the isomer was 0.006 at 3130 Å. The only other product at 3130 Å. that was identified was carbon monoxide. At shorter wave lengths, in addition to these products, methane, C_2 and C_3 hydrocarbons, acetone and biacetyl were identified. Although the ultraviolet absorption spectrum of 5-hexen-2-one resembles that of 2-hexanone, its photochemical stability is similar to that of unsaturated carbonyl compounds with the double bond conjugated with the carbonyl group.

Introduction

The photochemistry of unsaturated carbonyl compounds in which the double bond and the carbonyl group are conjugated, has been the subject of several investigations.[2-4] Two features appear to be peculiar to all these compounds as compared to the corresponding saturated carbonyl compounds. These are (i) the shift in the ultraviolet spectrum toward longer wave lengths and (ii) the stability of these molecules toward photochemical decomposition. As an illustration of the latter, it may be mentioned that the quantum yield for the production of carbon monoxide from crotonaldehyde is only about 0.05 at 250° and 3130 Å.[5] The present study of the photochemistry of 5-hexen-2-one in the vapor phase is believed to be the first one on an unsaturated carbonyl compound with an isolated double bond. In this instance, the ultraviolet spectrum was not expected to be

(1) This research was supported in part by Contract AF18(600) 1528 with the United States Air Force through the Air Force Office of Scientific Research of the Air Research and Development Command. Reproduction in whole or in part is permitted for any purpose by the United States Government.

(2) W. A. Noyes, Jr., and P. A. Leighton, "The Photochemistry of Gases," Reinhold Publishing Co., New York, N. Y., 1941, p. 351.

(3) E. W. R. Steacie, "Atomic and Free Radical Reactions," Reinhold Publishing Co., New York, N. Y., 1954, p. 317, 369.

(4) R. S. Tolberg and J. N. Pitts, Jr., THIS JOURNAL, **80**, 1304 (1958).

(5) J. N. Pitts, Jr., D. D. Thompson and R. W. Woolfolk, quoted by J. N. Pitts, Jr., *J. Chem. Educ.*, **34**, 112 (1957).